4-Aryliden-2-methyloxazol-5(4*H*)-one as a new scaffold for selective reversible MAGL inhibitors

Carlotta Granchi,[†] *Flavio Rizzolio,*[‡] *Vittorio Bordoni,*[†] *Isabella Caligiuri,*[‡] *Clementina Manera,*[†] *Marco Macchia,*[†] *Filippo Minutolo,*[†] *Adriano Martinelli,*[†] *Antonio Giordano,*[‡] *Tiziano Tuccinardi,**[†,‡]

Department of Pharmacy, University of Pisa, 56126 Pisa, Italy, Sbarro Institute for Cancer Research and Molecular Medicine Center for Biotechnology, Temple University Philadelphia PA 19122, USA.

AUTHOR INFORMATION

Corresponding Author

*Corresponding author phone: +39 0502219595; e-mail: tiziano.tuccinardi@farm.unipi.it

† University of Pisa

‡ Sbarro Institute for Cancer Research and Molecular Medicine Center for Biotechnology

Keywords. MAGL, Monoacylglycerol lipase, MAGL inhibitors, Monoacylglycerol lipase inhibitors, Hydrolase

ABSTRACT

This study reports on a preliminary structure-activity relationship exploration of 4-aryliden-2-methyloxazol-5(4*H*)-one-based compounds as MAGL/FAAH inhibitors. Our results highlight that this scaffold may serve for the development of selective MAGL inhibitors. A 69-fold selectivity against MAGL over FAAH was achieved for compound **16b** (MAGL and FAAH IC_{50} = 1.6 and 111 μM, respectively). Furthermore, the best compound behaved as a reversible ligand and showed promising antiproliferative activity in cancer cells.

Introduction

The endocannabinoid system is involved in a large number of physiopathological processes, such as the regulation of cellular proliferation, pain sensation, appetite and cognition[1]. It is widespread in the mammalian tissues and it acts as a pro-homeostatic effector being activated following transient or chronic perturbation of homeostasis and locally regulating the levels and action of other chemical signals[2]. Among the various reported endogenous lipids with endocannabinoid-like activity, 2-arachidonoylglycerol (2-AG) and arachidonoylethanolamide (AEA) are considered the two most important ligands of the CB_1 and CB_2 cannabinoid receptors. The signaling functions of AEA and 2-AG are terminated by enzymatic hydrolysis, which is mainly mediated by the fatty acid amide hydrolase (FAAH) and monoacylglicerol lipase (MAGL), respectively[3]. The *in vivo* cannabinometic effects of the endocannabinoids are rather weak, due to the fact that they are rapidly inactivated by cellular reuptake followed by intracellular hydrolysis. However, an increase in the level of endocannabinoids, caused by a reduction of their metabolism promoted by FAAH or MAGL, could lead to several advantageous effects[4]. MAGL inhibition in the periphery produces CB_1-dependent antinociceptive effects of noxious chemical, inflammatory, thermal, and neuropathic pain in mouse models[5]. Genetic and pharmacological blockades of MAGL also exhibit anti-inflammatory effects in the brain and neuroprotective effects for Parkinson's and Alzheimer's disease in mouse models[6]. Furthermore, other studies demonstrated that the inhibition of MAGL also exerts anti-anxiety

responses[7] and can be useful for modulating opiate drug dependence[8]. Finally, MAGL is upregulated in aggressive cancer cells and primary tumors and its inhibition in aggressive breast, ovarian, and melanoma cancer cells impairs cell migration, invasiveness, and tumorigenicity[9].

Three different types of MAGL inhibitors have been reported in literature so far: *1)* compounds that bind the enzyme covalently and irreversibly; *2)* compounds that bind covalently and reversibly; *3)* compounds that bind non-covalently. Among the compounds that bind covalently, two different sub-types are reported, those that bind the nucleophilic serine 122 (S122) and those that target the cysteines of the enzyme[3]. This last class of MAGL inhibitors generally shows a high selectivity against FAAH; however, this selectivity over other enzymes containing cysteine residues in the binding site still needs to be verified. Regarding the MAGL inhibitors that bind the nucleophilic S122, a wide number of compounds have been reported in literature, but only few show high selectivity against FAAH. One of the most promising ligands was developed by Cravatt and co-workers, and it consists of a carbamate derivative that behaves as an irreversible nanomolar inhibitor (**JZL-184**, Figure 1) and displays a high selectivity for MAGL *versus* FAAH enzymes[10]. In the last 5 years this compound has been used as a reference molecule for a wide number of *in vitro* and *in vivo* experimental studies. Very recently, Laitinen and co-workers, by combining the 1,2,4-triazole leaving group together with the aromatic benzodioxolyl moiety, reported the development of compound **JJKK-048** (Figure 1)[11], which is probably the most active and selective irreversible MAGL inhibitor ever reported. **CAY10499** (Figure 1) is a known irreversible inhibitor of both MAGL and FAAH enzymes[12]. Although **CAY10499** is a carbamate-based inhibitor, just like many other compounds interacting with the enzymes of the endocannabinoid system, further studies revealed that the 5-methoxy-1,3,4-oxadiazol-2(3*H*)-one ring is the main responsible for MAGL inhibition. The structure-activity relationships of this compound and further MALDI- and SELDI-TOF mass spectrometry analyses of analogous compounds[12-13] strongly supported a covalent interaction of the 5-methoxy-1,3,4-oxadiazol-2(3*H*)-one moiety with the enzyme active site, which occurs by a nucleophilic attack of the hydroxyl group of the enzyme's catalytic serine to the

carbonyl atom of the inhibitor's oxadiazolone ring. The 1,3,4-oxadiazol-2(3*H*)-one heterocycle was also found in the scaffold of other MAGL and FAAH inhibitors; most of them, however, were completely unselective[14] or characterized by a low selectivity for MAGL *versus* FAAH, such as compound **1** (Figure 1), with IC_{50} values of 0.35 μM for MAGL and 6.3 μM for FAAH[15-16].

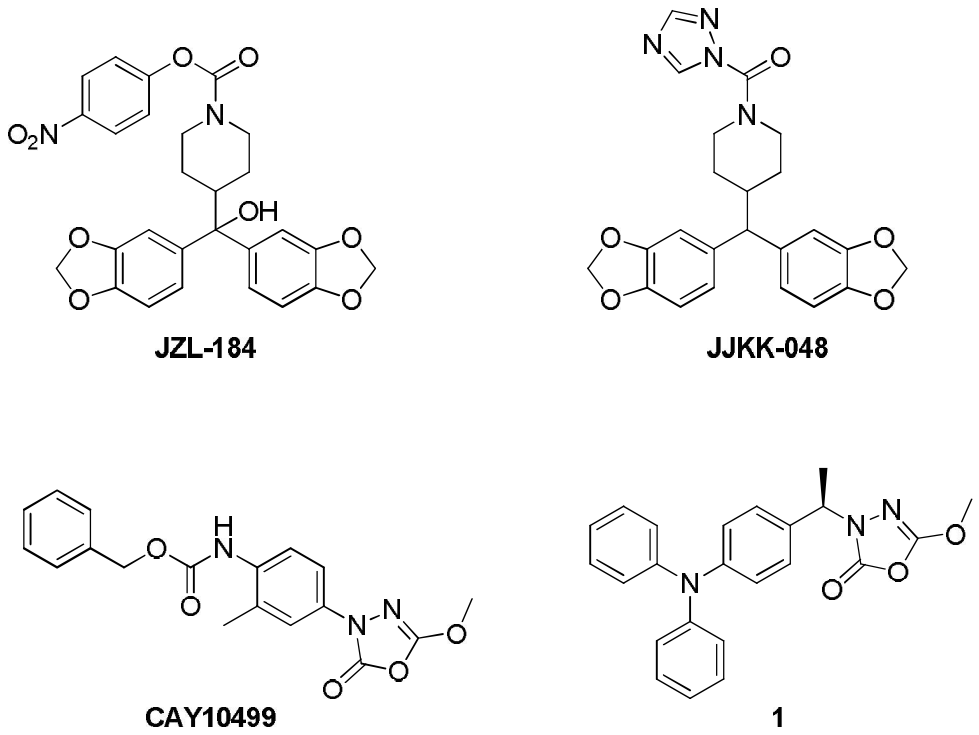

Figure 1. Structures of some of the most relevant MAGL inhibitors.

On the basis of the ability of the 5-methoxy-1,3,4-oxadiazol-2(3*H*)-one moiety (I, Figure 2) to interact with the catalytic serine of MAGL, we decided to design and synthesize compounds possessing a similar 2-methyl-4-methyleneoxazol-5(4*H*)-one scaffold (II, Figure 2). Both structures are based on a cyclic carbamate or lactone moiety, which can be opened in the presence of a nucleophile; moreover, the geometry of the C-N bond, in which the nitrogen atom is present in position 3 of the 5-methoxy-1,3,4-oxadiazol-2(3*H*)-one cycle, could be mimicked by the 4-arylidene portion of the 2-methyl-4-methyleneoxazol-5(4*H*)-one scaffold. Therefore, a series of three new exploratory small compounds **2**, **3** and **4** (Schemes 1 and 2), were initially synthesized to

determine which kind of aromatic portion (Ar, Figure 2), such as phenyl (**2**) or heteroaromatic five-membered cycle (**3** and **4**), was more suitable for obtaining good inhibition levels on MAGL. Further developments of this chemical class were carried out and nine new compounds (**16a-c**, **17a-c** and **18a-c**, Scheme 3) were obtained by introducing unsubstituted or *para*-substituted (fluoro and methoxy) phenyl rings in the aromatic ring of compound **2**. Finally, in order to verify whether the 2-methyloxazol-5(4*H*)-one moiety was necessary for the activity on MAGL, we synthesized and tested a compound containing the opened cycle (**19**, Scheme 4).

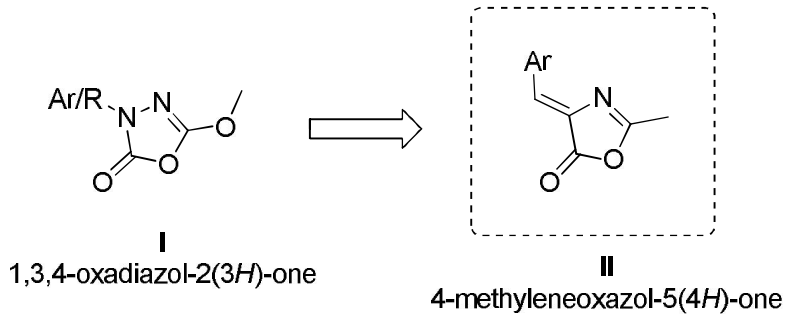

Figure 2. Design of the methyleneoxazol-5(4*H*)-one scaffold (II).

Results and discussion

Chemistry

The synthetic pathways for obtaining the target benzylidene-oxazolone compounds **2**, **3**, **4**, **16a-c**, **17a-c**, **18a-c** are outlined in Schemes 1, 2 and 3. Benzylidene-oxazolones were obtained in one step by Erlenmeyer-Plöchl condensation[17-18] of the appropriately substituted aromatic aldehydes with *N*-acetylglycine and sodium acetate in refluxing acetic anhydride. This reaction furnished only the thermodynamically stable (*Z*)-isomers in most cases, with the exception of heteroaromatic oxazolones **3** and **4**, which were obtained with a minimal percentage of the corresponding (*E*)-isomer, as detected by ^{1}H-NMR spectra (9% and 7% for **3** and **4**, respectively)[19]. Unlike

commercially available benzaldehyde **5** (Scheme 1) and 2-furaldehyde **6** (Scheme 2), pyrrole-2-carboxaldehyde **7** was subjected to the same condensation with *N*-acetylglycine but the desired oxazolone derivative **8** was not formed. In fact, under these conditions, only the heterocyclic nitrogen of **7** resulted as being acetylated, yielding compound **9**. After isolation and identification of **9**, it was again submitted to the same procedure to obtain the acetyl-pyrrol-methyloxazol-5(4*H*)-one **4** (Scheme 2). Attempts to obtain pyrrole derivative **8** from its acetylated analogue **4** were unsuccessful.

Scheme 1. Reagents and conditions: a) *N*-acetylglycine, Ac_2O, CH_3COONa, reflux, 5h.

Scheme 2. Reagents and conditions: a) *N*-acetylglycine, Ac_2O, CH_3COONa, reflux, 5h.

A series of phenyl-substituted analogues of compound **2** were prepared in order to investigate the effects caused by the variation of aromatic rings inserted in various positions on the phenyl of the promising compound **2** (see Biological evaluation section), in the light of the consideration that many of the known MAGL inhibitors simply consist of a lipophilic scaffold to which a heterocyclic system is bound. We therefore evaluated a series of slightly different lipophilic backbones linked to the same 2-methyloxazol-5(4*H*)-one moiety. Commercially available *ortho*-, *meta*- and *para*-bromo-substituted benzaldehydes **10-12** were subjected to a Pd-catalyzed cross-coupling reaction under classical Suzuki conditions (Scheme 3)[20]. In particular, bromo-derivatives **10-12** were treated with the appropriate unsubstituted (R_1 = H; Scheme 3) or *para*-substituted (R_1 = fluoro, methoxy; Scheme 3) phenylboronic acids under conventional heating at 100 °C, producing the desired arylsubstituted aldehydes **13a-c**, **14a-c** and **15a-c** in good yields (Scheme 3), which then followed the same condensation reaction seen before (Scheme 1) for the formation of the oxazolone cycle to obtain compounds **16a-c**, **17a-c** and **18a-c**.

S

cheme 3. Reagents and conditions: a) appropriately substituted phenylboronic acid, $Pd(OAc)_2$, PPh_3, aq. 2M Na_2CO_3, toluene, EtOH, 100 °C, 24 h; b) *N*-acetylglycine, Ac_2O, CH_3COONa, reflux, 5h.

Moreover, in order to further support the hypothesized action mechanism of these MAGL inhibitors, the oxazolone ring of the representative compound **18a** was opened to verify the key role played by the cyclic portion of these compounds in alkylating the enzyme's catalytic serine by opening the lactone ring. Therefore, compound **18a** was hydrolyzed under basic conditions, followed by acidification to obtain biphenylacetamidoacrylic acid derivative **19**[21], which was then submitted to biological assays as a valuable tool for establishing the pharmacophoric portion needed for MAGL inhibition (Scheme 4).

Scheme 4. Reagents and conditions: a) NaOH 1N, 90 °C, then HCl 3N, 0 °C.

Biological evaluation.

The inhibitory effects of the newly synthesized compounds on human isoforms of MAGL and FAAH (*h*MAGL and *h*FAAH) are reported in Table 1, together with those of two reference inhibitors (**CAY10499** and **JZL-184**). Among the three smallest compounds **2-4**, phenyl-substituted compound **2** displayed the most promising activity against MAGL (IC_{50} = 24.1 μM) and an unexpectedly high selectivity against FAAH, showing no detectable activity on this enzyme. Differently, **3** and **4** were weak MAGL inhibitors and inactive on FAAH. Encouraged by these first results, the series of differently substituted (*Z*)-biphenyl derivatives **16a-c**, **17a-c** and **18a-c** were tested. All the reported compounds showed IC_{50} values in the range of 1.0-2.2 μM on MAGL and a FAAH inhibitory activity in the range of 33.9-111 μM. The position of the distal phenyl and the *para*-substituent present on this ring did not seem to significantly influence the activity of the resulting compounds. Very interestingly, even if these compounds are not very potent inhibitors, they showed a very high selectivity ratio for MAGL *versus* FAAH, comparable to that observed for **JZL-184**, one of the most active and selective MAGL inhibitors currently available (see Table 1)[10]. In particular, among the *ortho*-biphenyl derivatives, the *para*-fluoro compound **16b** was the most selective inhibitor (69-fold, IC_{50} MAGL = 1.6 μM, IC_{50} FAAH = 111 μM). In order to verify the importance of the 2-methyl-4-methyleneoxazol-5(4*H*)-one ring for the interaction of these compounds with enzyme, compound **19**, the analogue of **18a** with the oxazolone ring open, was tested under the same conditions. This acetamidoacetic acid derivative showed a substantial loss of

MAGL inhibitory activity, thus supporting the importance of the oxazolone ring for interaction with the enzyme.

Table 1. Experimental inhibition activity (IC_{50}) on human MAGL and FAAH of the analyzed compounds.

#	MAGL IC_{50} (μM)	FAAH IC_{50} (μM)	Selectivity
2	24.1 ± 0.2	> 200	> 20
3	116 ± 7	> 200	> 2
4	> 200	> 200	/
16a	2.1 ± 0.3	94.0 ± 3.7	45
16b	1.6 ± 0.2	111 ± 7	69
16c	2.2 ± 0.2	33.9 ± 0.0	15
17a	1.2 ± 0.1	52.3 ± 3.6	44
17b	1.1 ± 0.1	69.1 ± 5.3	63
17c	1.0 ± 0.1	48.9 ± 0.8	49
18a	1.1 ± 0.1	45.4 ± 2.0	41
18b	1.7 ± 0.1	67.3 ± 2.8	40
18c	1.3 ± 0.1	37.3 ± 6.8	29
19	> 200	> 200	/
CAY10499	0.144 ± 0.003	0.014 ± 0.001	0.1
JZL-184	0.049 ± 0.004	3.3 ± 0.2	67

Furthermore, in order to verify if the compounds could interact with cysteines of the MAGL enzyme, the activity of the most selective compound **16b** was also tested in the presence of the thiol-containing agent 1,4-dithio-DL-threitol (DTT)[22]. As shown in Figure 3A, the *h*MAGL-IC_{50} value of compound **16b** was only very slightly influenced by the presence of DTT, shifting from 1.7 μM in the absence of DTT to 2.0 μM when assayed with 10 μM DTT, thus excluding the interaction of these compounds with the cysteine residues of the MAGL enzyme. In order to study the inhibition mechanism of the new reported compounds, the effects of dilution and preincubation on the inhibitory ability of compound **16b** were evaluated. In the dilution experiments, if **16b** is an irreversible inhibitor, then its inhibition potency should not drop upon dilution, whereas inhibition levels should be substantially reduced upon dilution in the presence of a reversible compound. As shown in Figure 3B, **16b** showed reversible inhibition, since the inhibition produced by 40 μM of

the compound was significantly higher compared with the inhibition observed with a 40X dilution, which appears similar to that produced by a 1 μM concentration of the compound. In order to further support these results, the activity of **16b** was tested at different preincubation times of the inhibitor with the enzyme. In principle, an irreversible inhibitor will increase its capacity to block the enzyme with increasingly longer incubation times in the presence of the enzyme prior to addition of the substrate; a constant IC_{50} value, conversely, supports a reversible mechanism[23]. As expected, compound **16b** did not show any significant increase in its ability to block MAGL activity after 30 and 60 minutes (Figure 3C), suggesting that its binding to MAGL is reversible.

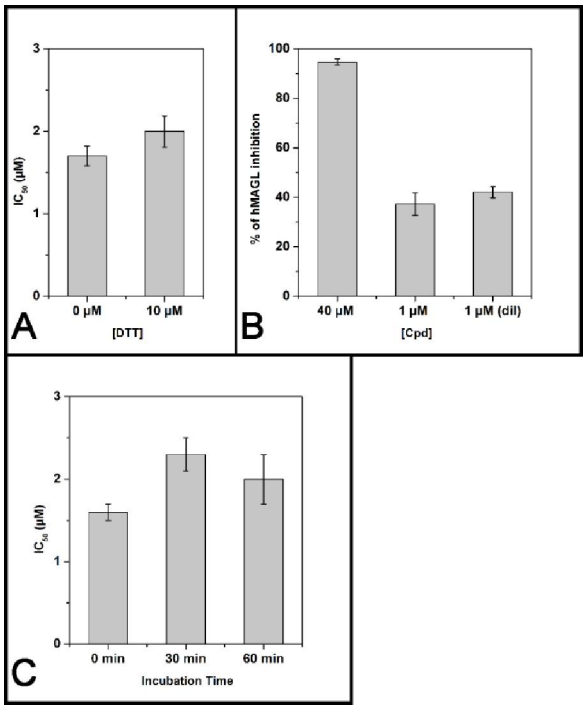

Figure 3. Compound **16b**-*h*MAGL inhibition analysis. A) Effect of DTT on the *h*MAGL inhibition properties. B) Dilution assay: the first two columns indicate the inhibition percentage of compound **16b** at a concentration of 40 μM and 1 μM. The third column indicates the inhibition percentage of compound **16b** after dilution (final concentration = 1 μM). C) IC_{50} (μM) values of **16b** at different preincubation times with *h*MAGL (0 min, 30 min and 60 min).

Compounds **16b**, **17b** and **18b** were also selected for *in vitro* experiments to evaluate their antiproliferative potency on selected cancer cells. Four tumor cell lines were chosen: the human breast MDA-MB-231 and MCF-7, and the human ovarian cancer cells COV318 and OVCAR-3. These cell lines were selected because of the critical role of MAGL in the tumor progression of breast and ovarian cancers[23-24]. All three compounds produced appreciable inhibition of cell viability, with IC_{50} values ranging from 10.0 to 54.4 μM (see Table 2). When compared to the covalent reference inhibitors **JZL-184** and **CAY10499**, compounds **16b-18b** showed similar activity profiles, and compound **16b** demonstrated an even better overall cytotoxicity on the ovarian cell lines, thus supporting the hypothesis that a reversible MAGL inhibition mechanism could be considered as an interesting approach for studying the MAGL inhibition effects on cancer cell proliferation.

Table 2. Cell growth inhibitory activities (IC_{50}) of compounds

	IC_{50} (μM)			
#	**MCF-7**	**MB-231**	**COV318**	**OVCAR-3**
16b	18.1 ± 2.8	42.1 ± 4.2	42.1 ± 5.1	10.0 ± 1.9
17b	15.8 ± 2.3	38.1 ± 4.2	50.5 ± 6.1	28.8 ± 3.5
18b	23.7 ± 1.8	54.4 ± 4.8	50.2 ± 5.1	18.0 ± 3.2
JZL-184	26.0 ± 5.1	37.8 ± 5.0	56.6 ± 3.2	52.9 ± 5.7
CAY10499[a]	4.2 ± 1.2	46.0 ± 6.9	106.7 ± 21.5	79.8 ± 11.7

[a] Ref 23

Docking studies.

The three most promising ligands (**16b**, **17b** and **18b**) and **CAY10499** were docked into human MAGL and humanized-rat FAAH using GOLD 5.1[25]. This docking analysis can help to analyze the interaction of the compounds before the formation of the covalent bond with the catalytic serine, thus highlighting the most important interactions for ligand recognition. In human MAGL, the 2-methyloxazolone rings of all three new compounds were placed near the catalytic S122, with the formation of one H-bond with the hydroxyl group of the serine and a second H-bond with the

nitrogen backbone of A51 (see Figure 4). For all three ligands, the benzylidene fragment acted as a linker, without showing important interactions, but allowing the interaction of the *p*-fluorophenyl ring into a lipophilic pocket mainly delimited by M88, L176, G177, P178, I179 and L205. The oxadiazolone ring of the reference compound **CAY10499** showed a very similar disposition to that of the 2-methyloxazolone ring of **16b**, **17b** and **18b**, with the two H-bonds with the hydroxyl group of S122 and the nitrogen backbone of A51. Similarly to **16b**, **17b** and **18b**, the 3-methylphenyl central portion of the molecule did not show important interactions with the protein, but allowed the proper localization of the benzylcarbamate portion in a lipophilic pocket mainly delimited by L148, A151, L213, L214, and V217 (see Figure 4D).

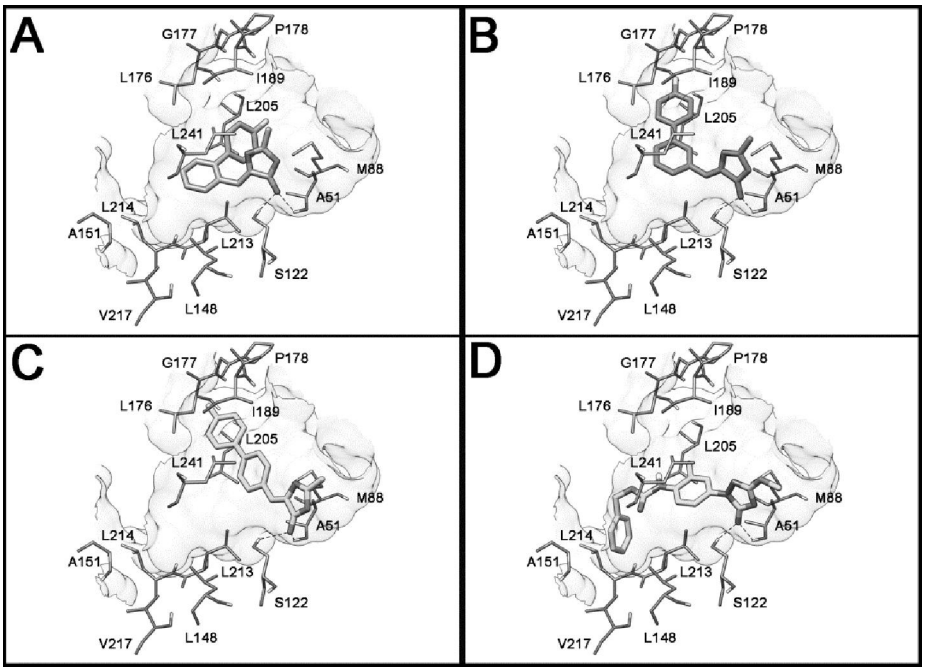

Figure 4. Docking of **16b** (A), **17b** (B), **18b** (C), and **CAY10499** (D) into the human MAGL receptor.

Figure 5A shows the docking of compound **CAY10499** into humanized-rat FAAH. Similarly to what was observed with the MAGL binding site and in considerable agreement with its good inhibitory activity on both enzymes, the oxadiazolone ring of this compound was placed near the

catalytic S241 with the formation of one H-bond with the hydroxyl group of the serine and a second H-bond with the nitrogen backbone of I238. The 3-methylphenyl central portion of the molecule showed lipophilic interactions with F192 and F244, whereas the benzylcarbamate fragment showed lipophilic interactions with Y194, L401 and L404. Conversely, the binding site shape of FAAH does not seem to allow the interaction of the 2-methyloxazolone ring of compounds **16b**, **17b** and **18b** in proximity to the catalytic region of the enzyme (Figure 5), since all three compounds showed binding dispositions that are completely different from that observed in the MAGL binding site, and none of them allowed the interaction of the 2-methyloxazolone ring with the catalytic S241. The rigid geometry imposed by the (*Z*)-4-benzylidene-2-methyloxazol-5(4*H*)-one portion, which could not fit into the catalytic region of the FAAH enzyme, is probably the cause of the low activity shown by these compounds for FAAH and, therefore, the great selectivity for MAGL.

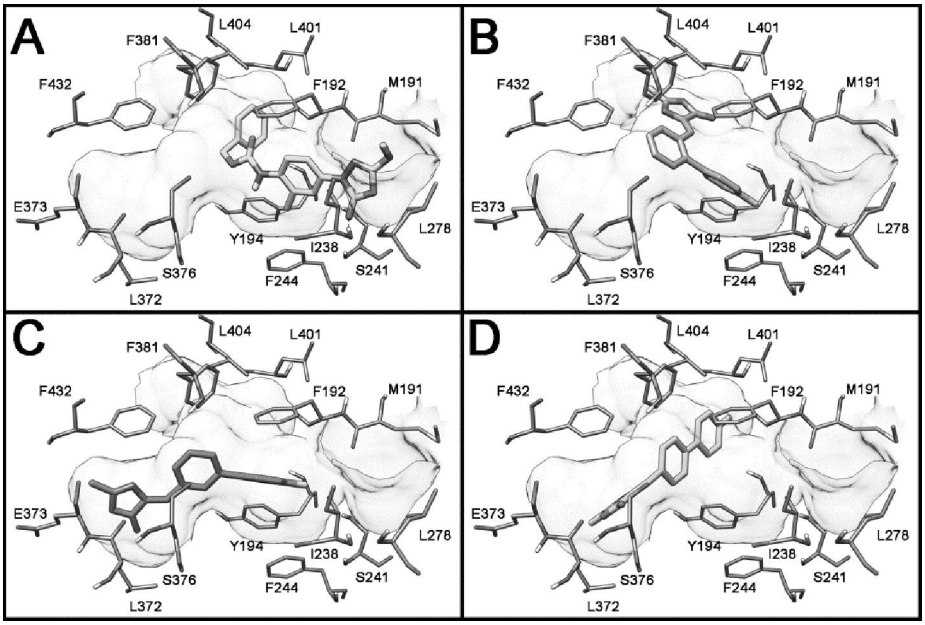

Figure 5. Docking of **CAY10499** (A), **16b** (B), **17b** (C), and **18b** (D) into humanized-rat FAAH receptor.

Conclusions.

Chanda and co-workers reported that the genetic MAGL inactivation in mouse models determined a dramatic reduction of the 2-AG hydrolase activity with the consequent presence of elevated 2-AG levels in the nervous system[26]. Furthermore, differently from FAAH, the chronic pharmacological blockade of MAGL determined receptor desensitization and pharmacological tolerance with cross-tolerance to CB_1 cannabinoid receptor agonists, impaired endocannabinoid-dependent synaptic plasticity and CB_1 brain receptor desensitization[27]. Taken together, these results could discourage the development of new MAGL inhibitors, however the use of low-doses of **JZL-184** induced anxiolytic-like effects that were also maintained after chronic treatment[28]. Chen *et al.*, by using an intermittent dosage regimen, obtained a significantly diminished amyloid neuropathology, reduced neuroinflammation and degeneration, and improved synaptic and cognitive function in animal model of Alzheimer's disease[29]. These two latter studies support the hypothesis that irreversible inhibition of MAGL should be avoided. Beyond the possibility of using a low or intermittent dosage regimen, a third way which has not yet been explored is the application of selective reversible MAGL inhibitors. In the present work we report a new class of MAGL inhibitors characterized by high selectivity, reversible properties and good activity in antiproliferative assays. Molecular modeling and SAR studies support the hypothesis that the key fragment for selectivity is the 2-methyloxazol-5(4*H*)-one scaffold. Further computational and synthetic efforts will be carried out in order to improve the activity and selectivity of the herein reported chemical class of MAGL inhibitors, in order to candidate them as new leads for *in vivo* inhibition of the MAGL enzyme.

Experimental protocols

Chemistry

General

Commercially available chemicals were purchased from Sigma-Aldrich or Alfa Aesar and used without further purification. PS-TsNHNH$_2$ was purchased from Argonaut Technologies Inc and **JZL-184** and **CAY10499** were purchased from Cayman Chemical. NMR spectra were obtained with a Bruker Avance III 400 MHz spectrometer. Chemical shifts (δ) are reported in parts per million downfield from tetramethylsilane and referenced from solvent references. Chromatographic separations were performed on silica gel columns by flash chromatography (Kieselgel 60, 0.040–0.063 mm; Merck). Reactions were followed by thin-layer chromatography (TLC) on Aldrich aluminum silica gel (F254) sheets that were visualized under a UV lamp. Evaporation was performed in vacuo (rotating evaporator). Sodium sulfate was always used as the drying agent.

*General procedure for the preparation of the oxazole derivatives **2, 3, 4, 16a-c, 17a-c, 18a-c**.*

A mixture of properly substituted aromatic aldehydes **5**, **6**, **9**, **13a-c**, **14a-c** or **15a-c** (1 eq), *N*-acetylglycine (1 eq) and sodium acetate (1 eq) in acetic anhydride (5 mL/5 mmol aldehyde) was stirred at reflux for 5 h and then warmed slowly to room temperature over 16 h. The reaction was quenched with water and extracted with AcOEt. The organic layer was washed sequentially with water and saturated brine, dried over Na_2SO_4 and the solvent was removed under reduced pressure. The residue was purified with a flash column chromatography using the indicated eluent and pure fractions containing the desired compound were evaporated to dryness affording the desired product.

*(Z)-4-Benzylidene-2-methyloxazol-5(4H)-one (**2**).*

yellow crystalline solid, yield: 47% (417.1 mg) from **5**. R_f = 0.14 (*n*-hexane/EtOAc 95:5).

^{1}H-NMR ($CDCl_3$, 400 MHz) δ (ppm): 2.41 (s, 3H), 7.15 (s, 1H), 7.42-7.47 (m, 3H), 8.07-8.09 (m, 2H).

^{13}C-NMR ($CDCl_3$, 100 MHz) δ (ppm): 15.84, 129.03 (3C), 131.28, 131.65, 132.31, 132.70, 133.27, 166.26, 167.97.

*(Z)-4-(Furan-2-ylmethylene)-2-methyloxazol-5(4H)-one (**3**).*

bright yellow crystalline solid, yield: 49% (451.2 mg) from **6**. R_f = 0.18 (*n*-hexane/EtOAc 9:1).

^{1}H-NMR ($CDCl_3$, 400 MHz) δ (ppm): 2.40 (s, 3H), 6.59 (dd, 1H, *J* = 3.6, 1.8 Hz), 7.03 (s, 1H), 7.28 (d, 1H, *J* = 3.6 Hz), 7.68 (d, 1H, *J* = 1.3 Hz). Signals attributed to the (*E*) isomer (9%): 2.34 (s, 3H), 6.62-6.63 (m, 1H), 7.63 (d, 1H, *J* = 1.5 Hz), 8.03 (d,1H, *J* = 3.6 Hz).

^{13}C-NMR ($CDCl_3$, 100 MHz) δ (ppm): 15.82, 113.57, 118.00, 120.17, 129.57, 147.06, 150.08, 165.88, 167.54.

*(Z)-4-((1-Acetyl-1H-pyrrol-2-yl)methylene)-2-methyloxazol-5(4H)-one (**4**).*

bright yellow crystalline solid, yield: 18% (68.0 mg) from **9**. R_f = 0.12 (*n*-hexane/Et_2O 6:4).

^{1}H-NMR ($CDCl_3$, 400 MHz) δ (ppm): 2.37 (s, 3H), 2.62 (s, 3H), 6.43 (t, 1H, *J* = 3.3 Hz), 7.30 (dd, 1H, *J* = 3.3, 1.4 Hz), 7.69-7.71 (m, 1H), 8.18 (s, 1H). Signals attributed to the (*E*) isomer (7%): 2.32 (s, 3H), 2.63 (s, 3H), 7.33 (dd, 1H, *J* = 3.3, 1.2 Hz), 8.40 (s, 1H).

^{13}C-NMR ($CDCl_3$, 100 MHz) δ (ppm): 15.79, 24.59, 114.13, 121.45, 124.54, 125.62, 130.38, 130.60, 165.25, 167.62, 169.53.

*1-Acetyl-1H-pyrrole-2-carbaldehyde (**9**).*

brown-orange solid, yield: 33% (94.0 mg) from **7**. R_f = 0.12 (*n*-hexane/ EtOAc 8:2).

^{1}H-NMR ($CDCl_3$, 400 MHz) δ (ppm): 2.66 (s, 3H), 6.36 (t, 1H, *J* = 3.3 Hz), 7.21 (dd, 1H, *J* = 3.6, 1.6 Hz), 7.33 (dd, 1H, *J* = 3.1, 1.6 Hz), 10.29 (s, 1H).

^{13}C-NMR ($CDCl_3$, 100 MHz) δ (ppm): 24.12, 112.97, 122.98, 126.75, 135.76, 169.24, 182.58.

*(Z)-4-([1,1'-Biphenyl]-2-ylmethylene)-2-methyloxazol-5(4H)-one (**16a**).*

yellow crystalline solid, yield: 16% (107.0 mg) from **13a**. R_f = 0.13 (*n*-hexane/EtOAc 9:1).

^{1}H-NMR ($CDCl_3$, 400 MHz) δ (ppm): 2.42 (s, 3H), 7.21 (s, 1H), 7.30-7.33 (m, 2H), 7.38- 7.50 (m, 6H), 8.65-8.69 (m, 1H).

^{13}C-NMR ($CDCl_3$, 100 MHz) δ (ppm): 15.84, 127.83, 128.04, 128.58 (2C), 130.06 (2C), 130.51, 130.53, 130.80, 130.96, 132.11, 132.80, 139.89, 145.08, 166.33, 167.70.

*(Z)-4-((4'-Fluoro-[1,1'-biphenyl]-2-yl)methylene)-2-methyloxazol-5(4H)-one (**16b**).*

bright yellow crystalline solid, yield: 24% (137.0 mg) from **13b**. R_f = 0.14 (*n*-hexane/EtOAc 95:5).

^{1}H-NMR ($CDCl_3$, 400 MHz) δ (ppm): 2.42 (s, 3H), 7.10-7.17 (m, 3H), 7.26-7.30 (m, 2H), 7.35-7.38 (m, 1H), 7.45-7.48 (m, 2H), 8.64-8.66 (m, 1H).

^{13}C-NMR ($CDCl_3$, 100 MHz) δ (ppm): 15.88, 115.67 (d, 2C, J = 21.1 Hz), 128.03, 130.04, 130.53, 130.87, 131.05, 131.68 (d, 2C, J = 8.0 Hz), 132.18, 133.02, 135.91 (d, J = 3.0 Hz), 143.93, 162.79 (d, J = 247.5 Hz), 166.57, 167.67.

*(Z)-4-((4'-Methoxy-[1,1'-biphenyl]-2-yl)methylene)-2-methyloxazol-5(4H)-one (**16c**).*

bright yellow crystalline solid, yield: 15% (83.3 mg) from **13c**. R_f = 0.18 (*n*-hexane/EtOAc 9:1).

^{1}H-NMR ($CDCl_3$, 400 MHz) δ (ppm): 2.42 (s, 3H), 3.87 (s, 3H), 6.98 (AA'XX', 2H, J_{AX} = 8.7 Hz, $J_{AA'/XX'}$ = 2.5 Hz), 7.22-7.25 (m, 3H), 7.37-7.42 (m, 1H), 7.44-7.48 (m, 2H), 8.62-8.64 (m, 1H).

^{13}C-NMR ($CDCl_3$, 100 MHz) δ (ppm):15.85, 55.50, 114.11 (2C), 127.48, 130.52, 130.83, 130.87, 131.01, 131.26 (2C), 132.13, 132.24, 132.64, 144.83, 159.62, 166.18, 167.81.

*(Z)-4-([1,1'-Biphenyl]-3-ylmethylene)-2-methyloxazol-5(4H)-one (**17a**).*

bright yellow crystalline solid, yield: 43% (530.0 mg) from **14a**. R_f = 0.15 (*n*-hexane/EtOAc 95:5).

^{1}H-NMR ($CDCl_3$, 400 MHz) δ (ppm): 2.42 (s, 3H), 7.21 (s, 1H), 7.39 (tt, 1H, J = 7.3, 1.5 Hz), 7.45-7.50 (m, 2H), 7.52 (t, 1H, J = 7.8 Hz), 7.61-7.67 (m, 3H), 8.08-8.11 (m, 1H), 8.28 (t, 1H, J = 1.7 Hz).

^{13}C-NMR ($CDCl_3$, 100 MHz) δ (ppm): 15.86, 127.33 (2C), 127.85, 129.04 (3C), 129.46, 130.03, 131.03, 131.48, 133.02, 133.77, 140.47, 142.05, 166.37, 167.95.

*(Z)-4-((4'-Fluoro-[1,1'-biphenyl]-3-yl)methylene)-2-methyloxazol-5(4H)-one (**17b**).*

white crystalline solid, yield: 45% (382.0 mg) from **14b**. R_f = 0.11 (*n*-hexane/EtOAc 95:5).

^{1}H-NMR ($CDCl_3$, 400 MHz) δ (ppm): 2.42 (s, 3H), 7.16 (double AA'XX', 2H, $^3J_{HF\text{-}o}$ = 9.8 Hz, J_{AX} = 8.7 Hz, $J_{AA'XX'}$ = 2.6 Hz), 7.20 (s, 1H), 7.51 (t, 1H, *J* = 7.7 Hz), 7.55-7.62 (m, 3H), 8.05-8.09 (m, 1H), 8.25 (t, 1H, *J* = 1.7 Hz).

^{13}C-NMR (Acetone-d_6, 100 MHz) δ (ppm): 15.67, 116.47, 116.69, 129.78 (d, 2C, *J* = 9.1 Hz), 130.13, 130.41 (d, 2C, *J* = 21.1 Hz), 131.45, 131.72, 134.37, 135.05, 137.48 (d, *J* = 2.0 Hz), 141.39, 163.61 (d, *J* = 244.5 Hz), 168.02, 168.19.

*(Z)-4-((4'-Methoxy-[1,1'-biphenyl]-3-yl)methylene)-2-methyloxazol-5(4H)-one (**17c**).*

After an initial purification, compound **17c** was obtained as a mixture with starting material **14c**, therefore this mixture dissolved in dry THF was stirred in the presence of polystyrene sulfonyl hydrazide (PS-$TsNHNH_2$, 3 eq relative to aldehyde, minimum capacity 2.2 mmol/g) until disappearance of the starting material. Then the reaction was filtered and washed with THF and the filtrate was evaporated and concentrated under vacuum, to afford a crude residue that was purified by column chromatography.

bright yellow crystalline solid, yield: 17% (94.7 mg) from **14c**. R_f = 0.21 (*n*-hexane/EtOAc 9:1).

^{1}H-NMR (Acetone-d_6, 400 MHz) δ (ppm): 2.42 (s, 3H), 3.86 (s, 3H), 7.06 (AA'XX', 2H, J_{AX} = 8.8 Hz, $J_{AA'XX'}$ = 2.6 Hz), 7.21 (s, 1H), 7.55 (t, 1H, *J* = 7.8 Hz), 7.66 (AA'XX', 2H, J_{AX} = 8.8 Hz, $J_{AA'XX'}$ = 2.6 Hz), 7.72 (dt, 1H, *J* = 7.8, 1.4 Hz), 8.18-8.20 (m, 1H), 8.43 (t, 1H, *J* = 1.7 Hz).

^{13}C-NMR (Acetone-d_6, 100 MHz) δ (ppm): 15.65, 55.66, 115.27, 128.87 (3C), 129.78, 130.16, 130.82, 131.07 (2C), 133.34, 134.17, 134.93, 142.11, 160.69, 167.83, 168.24.

*(Z)-4-([1,1'-Biphenyl]-4-ylmethylene)-2-methyloxazol-5(4H)-one (**18a**).*

bright yellow crystalline solid, yield: 47% (336.0 mg) from **15a**. R_f = 0.13 (*n*-hexane/EtOAc 95:5).

^{1}H-NMR ($CDCl_3$, 400 MHz) δ (ppm): 2.43 (s, 3H), 7.19 (s, 1H), 7.37-7.42 (m, 1H), 7.45-7.49 (m, 2H), 7.63-7.65 (m, 2H), 7.68-7.70 (m, 2H), 8.15-8.17 (m, 2H).

^{13}C-NMR ($CDCl_3$, 100 MHz) δ (ppm): 15.88, 127.30 (2C), 127.65 (2C), 128.26, 129.11 (2C), 131.21, 132.31, 132.61, 132.83 (2C), 140.17, 143.88, 166.17, 168.00.

*(Z)-4-((4'-Fluoro-[1,1'-biphenyl]-4-yl)methylene)-2-methyloxazol-5(4H)-one (**18b**).*

bright yellow crystalline solid, yield: 22% (154.0 mg) from **15b**. R_f = 0.18 (*n*-hexane/EtOAc 9:1).

^{1}H-NMR ($CDCl_3$, 400 MHz) δ (ppm): 2.43 (s, 3H), 7.14-7.19 (m, 3H), 7.60 (double AA'XX', 2H, $^4J_{HF\text{-}m}$ = 5.3 Hz, J_{AX} = 8.8 Hz, $J_{AA'/XX'}$ = 2.5 Hz), 7.61-7.65 (m, 2H), 8.13-8.17 (m, 2H).

^{13}C-NMR ($CDCl_3$, 100 MHz) δ (ppm): 15.86, 116.01 (d, 2C, J = 21.1 Hz), 127.46 (2C), 128.93 (d, 2C, J = 8.0 Hz), 130.98, 132.33, 132.72, 132.86 (2C), 136.30 (d, J = 4.0 Hz), 142.79, 163.08 (d, J = 247.5 Hz), 166.26, 167.92.

*(Z)-4-((4'-Methoxy-[1,1'-biphenyl]-4-yl)methylene)-2-methyloxazol-5(4H)-one (**18c**).*

bright yellow crystalline solid, yield: 23% (159.4 mg) from **15c**. R_f = 0.14 (*n*-hexane/EtOAc 9:1).

^{1}H-NMR ($CDCl_3$, 400 MHz) δ (ppm): 2.42 (s, 3H), 3.87 (s, 3H), 7.00 (AA'XX', 2H, J_{AX} = 8.8 Hz, $J_{AA'/XX'}$ = 2.6 Hz), 7.18 (s, 1H), 7.59 (AA'XX', 2H, J_{AX} = 8.8 Hz, $J_{AA'/XX'}$ = 2.6 Hz), 7.64 (AA'XX', 2H, J_{AX} = 8.5 Hz, $J_{AA'/XX'}$ = 1.8 Hz), 8.11-8.15 (m, 2H).

^{13}C-NMR ($CDCl_3$, 100 MHz) δ (ppm): 15.84, 55.53, 114.57 (2C), 127.04 (2C), 128.37 (2C), 131.33, 131.69, 132.28, 132.55, 132.86 (2C), 143.48, 160.00, 165.92, 168.04.

*General procedure for the formation of biphenyl derivatives **13a-c**, **14a-c** and **15a-c**.*

A solution of $Pd(OAc)_2$ (0.03 eq) and triphenylphosphine (0.15 eq) in ethanol (6 mL/2.7 mmol bromo-derivative) and toluene (6 mL/2.7 mmol bromo-derivative) was stirred at RT under nitrogen

for 10 min. After that period, commercially available bromo-substituted aldehydes **10-12** (1 eq), 2M aqueous Na_2CO_3 (6 mL/2.7 mmol bromo-derivative), and the appropriate substituted phenylboronic acid (1.6 eq) were sequentially added. The resulting mixture was heated at 100 °C in a sealed vial under nitrogen for 24 h. After being cooled to RT, the mixture was diluted with water and extracted with EtOAc. The combined organic phase were dried and concentrated. The crude product was purified by flash chromatography using the indicated eluent and pure fractions containing the desired biphenyl compound were evaporated to dryness affording the desired product.

*[1,1'-Biphenyl]-2-carbaldehyde (**13a**).*

yellow oil, yield: 76% (490.3 mg) from aldehyde **10** and phenylboronic acid. R_f = 0.16 (*n*-hexane/EtOAc 98:2).

^{1}H-NMR ($CDCl_3$, 400 MHz) δ (ppm): 7.38-7.40 (m, 2H), 7.44-7.53 (m, 5H), 7.65 (td, 1H, J = 7.5, 1.5 Hz), 8.04 (ddd, 1H, J = 7.8, 1.4, 0.4 Hz), 9.99 (s, 1H).

*4'-Fluoro-[1,1'-biphenyl]-2-carbaldehyde (**13b**).*

white solid, yield: 99% (619.3 mg) from aldehyde **10** and 4-fluorophenylboronic acid. R_f = 0.20 (*n*-hexane/EtOAc 95:5).

^{1}H-NMR ($CDCl_3$, 400 MHz) δ (ppm): 7.17 (double AA'XX', 2H, $^3J_{HF\text{-}o}$ = 9.5 Hz, J_{AX} = 8.6 Hz, $J_{AA'/XX'}$ = 2.5 Hz), 7.36 (double AA'XX', 2H, $^4J_{HF\text{-}m}$ = 5.3 Hz, J_{AX} = 8.6 Hz, $J_{AA'/XX'}$ = 2.5 Hz), 7.42 (dd, 1H, J = 7.7, 0.7 Hz), 7.48-7.53 (m, 1H), 7.64 (td, 1H, J = 7.5, 1.4 Hz), 8.02 (dd, 1H, J = 7.8, 1.3 Hz), 9.97 (s, 1H).

*4'-Methoxy-[1,1'-biphenyl]-2-carbaldehyde (**13c**).*

light yellow oil, yield: 99% (667.7 mg) from aldehyde **10** and 4-methoxyphenylboronic acid. R_f = 0.14 (*n*-hexane/EtOAc 95:5).

^{1}H-NMR ($CDCl_3$, 400 MHz) δ (ppm): 3.88 (s, 3H), 7.01 (AA'XX', 2H, J_{AX} = 8.8 Hz, $J_{AA'/XX'}$ = 2.5 Hz), 7.31 (AA'XX', 2H, J_{AX} = 8.7 Hz, $J_{AA'/XX'}$ = 2.5 Hz), 7.42-7.49 (m, 2H), 7.62 (td, 1H, J = 7.5, 1.4 Hz), 8.00 (dd, 1H, J = 7.8, 1.4 Hz), 10.00 (s, 1H).

*[1,1'-Biphenyl]-3-carbaldehyde (**14a**).*

light yellow oil, yield: 88% (868.0 mg) from aldehyde **11** and phenylboronic acid. R_f = 0.28 (*n*-hexane/EtOAc 95:5).

^{1}H-NMR ($CDCl_3$, 400 MHz) δ (ppm): 7.40 (tt, 1H, J = 7.3, 1.6 Hz), 7.46-7.51 (m, 2H), 7.59-7.65 (m, 3H), 7.85-7.89 (m, 2H), 8.11 (t, 1H, J = 1.5 Hz), 10.10 (s, 1H).

*4'-Fluoro-[1,1'-biphenyl]-3-carbaldehyde (**14b**).*

colorless oil, yield: 99% (668.9 mg) from aldehyde **11** and 4-fluorophenylboronic acid. R_f = 0.14 (*n*-hexane/EtOAc 95:5).

^{1}H-NMR ($CDCl_3$, 400 MHz) δ (ppm): 7.17 (double AA'XX', 2H, $^3J_{HF\text{-}o}$ = 9.8, Hz, J_{AX} = 8.7 Hz, $J_{AA'/XX'}$ = 2.6 Hz), 7.56-7.63 (m, 3H), 7.81 (ddd, 1H, J = 7.8, 1.9, 1.2 Hz), 7.86 (dt, 1H, J = 7.6, 1.4 Hz), 8.05 (t, 1H, J = 1.6 Hz), 10.09 (s, 1H).

*4'-Methoxy-[1,1'-biphenyl]-3-carbaldehyde (**14c**).*

white crystalline solid, yield: 99% (791.0 mg) from aldehyde **11** and 4-methoxyphenylboronic acid. R_f = 0.12 (*n*-hexane/EtOAc 95:5).

^{1}H-NMR ($CDCl_3$, 400 MHz) δ (ppm): 3.87 (s, 3H), 7.01 (AA'XX', 2H, J_{AX} = 8.9 Hz, $J_{AA'/XX'}$= 2.6 Hz), 7.55-7.60 (m, 3H), 7.80-7.84 (m, 2H), 8.06 (t, 1H, J = 1.6 Hz), 10.08 (s, 1H).

*[1,1'-Biphenyl]-4-carbaldehyde (**15a**).*

light yellow solid, yield: 92% (909.8 mg) from aldehyde **12** and phenylboronic acid. R_f = 0.23 (*n*-hexane/EtOAc 95:5).

^{1}H-NMR ($CDCl_3$, 400 MHz) δ (ppm): 7.42 (td, 1H, J = 7.3, 1.7 Hz), 7.46-7.52 (m, 2H), 7.63-7.66 (m, 2H), 7.76 (AA'XX', 2H, J_{AX} = 8.4 Hz, $J_{AA'/XX'}$= 2.1 Hz), 7.96 (AA'XX', 2H, J_{AX} = 8.4 Hz, $J_{AA'/XX'}$= 1.7 Hz), 10.06 (s, 1H).

*4'-Fluoro-[1,1'-biphenyl]-4-carbaldehyde (**15b**).*

white solid, yield: 98% (527.2 mg) from aldehyde **12** and 4-fluorophenylboronic acid. R_f = 0.17 (*n*-hexane/EtOAc 95:5).

^{1}H-NMR ($CDCl_3$, 400 MHz) δ (ppm): 7.17 (double AA'XX', 2H, $^3J_{HF\text{-}o}$ = 9.7, Hz, J_{AX} = 8.7 Hz, $J_{AA'/XX'}$ = 2.6 Hz), 7.61 (double AA'XX', 2H, $^4J_{HF\text{-}m}$ = 5.3, Hz, J_{AX} = 8.9 Hz, $J_{AA'/XX'}$ = 2.6 Hz), 7.70 (AA'XX', 2H, J_{AX} = 8.2 Hz, $J_{AA'/XX'}$= 1.7 Hz), 7.95 (AA'XX', 2H, J_{AX} = 8.5 Hz, $J_{AA'/XX}$= 1.8 Hz), 10.06 (s, 1H).

*4'-Methoxy-[1,1'-biphenyl]-4-carbaldehyde (**15c**).*

white solid, yield: 95% (542.0 mg) from aldehyde **12** and 4-methoxyphenylboronic acid. R_f = 0.18 (*n*-hexane/EtOAc 95:5).

^{1}H-NMR ($CDCl_3$, 400 MHz) δ (ppm): 3.87 (s, 3H), 7.01 (AA'XX', 2H, J_{AX} = 8.9 Hz, $J_{AA'/XX'}$= 2.6 Hz), 7.60 (AA'XX', 2H, J_{AX} = 8.9 Hz, $J_{AA'/XX'}$= 2.6 Hz), 7.72 (AA'XX', 2H, J_{AX} = 8.2 Hz, $J_{AA'/XX'}$= 1.7 Hz), 7.93 (AA'XX', 2H, J_{AX} = 8.5 Hz, $J_{AA'/XX}$= 1.8 Hz), 10.04 (s, 1H).

*Procedure for synthesis of compound (Z)-3-([1,1'-biphenyl]-4-yl)-2-acetamidoacrylic acid (**19**).*

A suspension of azlactone **18a** (150 mg, 0.570 mmol) in 1.5 mL of 1 N sodium hydroxide solution was heated at 90 °C until homogeneous. The clear solution was cooled in an ice bath and then was acidified to pH 1-2 with a hydrochloric acid solution 3 N and a white precipitate was formed. The precipitate thus formed was isolated by filtration and washed with distilled water. The precipitate was then dissolved in acetone, dried, filtered and evaporated under reduced pressure to obtain a

white solid. The solid was further purified by crystallization in *n*-hexane/EtOAc to afford the pure desired compound **19** in 14% yield (21.8 mg) as white crystals.

^{1}H-NMR (DMSO-d_6, 400 MHz) δ (ppm): 2.01 (s, 3H), 7.26 (s, 1H), 7.36-7.41 (m, 1H), 7.46-7.50 (m, 2H), 7.69-7.74 (m, 6H), 9.53 (bs, 1H), 12.66 (bs, 1H).

^{13}C-NMR (DMSO-d_6, 100 MHz) δ (ppm): 22.56, 126.61 (2C), 126.66 (2C), 127.36, 127.82, 129.01 (3C), 130.35, 130.50, 132.88, 139.26, 140.53, 166.37, 169.13.

Biological evaluation

MAGL inhibition assay

Human recombinant MAGL, and 4-nitrophenylacetate substrate (4-NPA) were from Cayman Chemical. The IC_{50} values for compounds were generated in 96-well microtiter plates. The MAGL reaction was conducted at room temperature at a final volume of 200 µL in 10 mM Tris buffer, pH 7.2, containing 1 mM EDTA. A total of 150 µL of 4-NPA 133.3 µM (final concentration = 100 µM) was added to 10 µL of DMSO containing the appropriate amount of compound. The reaction was initiated by the addition of 40 µL of MAGL (11 ng/well) in such a way that the assay was linear over 30 min. The final concentration of the analyzed compounds ranged for **CAY10499** and **JZL-184** from 10 to 0.00001 µM and for the synthesized compounds from 200 to 0.0128 µM. After the reaction had proceeded for 30 min, absorbance values were then measured by using a VictorX3 PerkinElmer instrument at 405 nm. Two reactions were also run: one reaction containing no compounds and the second one containing neither inhibitor nor enzyme. IC_{50} values were derived from experimental data using the Sigmoidal dose–response fitting of GraphPad Prism software. To remove possible false positive results, for each compound concentration a blank analysis was carried out, and the final absorbance results were obtained detracting the absorbance produced by the presence of all the components except MAGL in the same conditions.

DTT interference assay

The inhibition assay was the same described above, with the exception that prior to the addition of 40 μL of MAGL (11 ng/well), the compound-substrate mixture was incubated 15 min in the presence of DTT at a 10 μM concentration.

MAGL preincubation assay

The MAGL reaction was conducted at room temperature at a final volume of 200 μL in 10 mM Tris buffer, pH 7.2, containing 1 mM EDTA. A total of 150 μL of MAGL (11 ng/well) was added to 10 μL of DMSO containing the appropriate amount of compound. After 0 min, 30 min, and 60 min of incubation time the reaction was initiated by the addition of 40 μL of 4-NPA 500 μM. The enzyme activity was then measured according to the procedure described above.

MAGL dilution assay

The enzyme (880 ng in 75 μL of Tris buffer, pH 7.2) was incubated during 60 min at room temperature with 5 μL of compound **16b** (concentration of 40 μM in the mixture) dissolved in DMSO. The MAGL-inhibitor mixture was then diluted 40-fold with the buffer. After 15 min of incubation, the reaction was initiated on a 160 μL aliquot by the addition of 40 μL of 4-NPA 500 μM and the enzyme activity was measured according to the procedure described above.

FAAH inhibition assay

The IC_{50} values for compounds were generated in 96-well microtiter plates. The FAAH reaction was conducted at room temperature at a final volume of 200 μL in 125 mM Tris buffer, pH 9.0, containing 1 mM EDTA. A total of 150 μL of AMC arachidonoylamide 13.3 μM (final concentration = 10 μM) was added to 10 μL of DMSO containing the appropriate amount of compound. The reaction was initiated by the addition of 40 μL of FAAH (0.9 μg/well) in such a way that the assay was linear over 30 min. The final concentration of the analyzed compounds

ranged for **CAY10499** from 10 to 0.00001 μM and for the other compounds from 200 to 0.0128 μM. After the reaction had proceeded for 30 min, fluorescence values were then measured by using a VictorX3 PerkinElmer instrument at an excitation wavelength of 340 nm and an emission of 460 nm. Two reactions were also run: one reaction containing no compounds and the second one containing neither inhibitor nor enzyme. IC_{50} values were derived from experimental data using the Sigmoidal dose–response fitting of GraphPad Prism software. To remove possible false positive results, for each compound concentration a blank analysis was carried out, and the final fluorescence results were obtained detracting the fluorescence produced by the presence of all the components except FAAH in the same conditions.

Cell viability assay

MDA-MB-231, MCF-7, COV318, and OVCAR-3 (from ATCC) were maintained at 37 °C in a humidified atmosphere containing 5% CO_2 accordingly to the supplier. Normal (1.5×10^4) and tumor (5×10^2) cells were plated in 96-well culture plates. The day after seeding, vehicle or compounds were added at different concentrations to the medium. Compounds were added to the cell culture at a concentration ranging from 200 to 0.02 μM. Cell viability was measured after 96 h according to the supplier (Promega, G7571) with a Tecan F200 instrument. IC_{50} values were calculated from logistical dose response curves. Averages were obtained from three independent experiments, and error bars are standard deviations (n = 3).

Docking Studies

The ligands were built by means of Maestro[30] and were then minimized in a water environment (using the generalized Born/surface area model) by means of Macromodel[31]. They were minimized using the conjugate gradient, the MMFFs force field, and a distance-dependent dielectric constant of 1.0 until they reached a convergence value of 0.05 kcal $Å^{-1}$ mol^{-1}. The ligands were docked using GOLD 5.1[25] in the human MAGL (3JWE[32] PDB code) and the humanized-rat FAAH (3LJ7[33]

PDB code). The region of interest used by the docking software was defined in such a manner that it contained all the residues that stayed within 15 Å from the ligand in the X-ray structures; the possibility for the ligand to flip ring corners was activated, while the 'allow early termination' command was deactivated. For all the other parameters, the GOLD default ones were used, and the ligands were submitted to 30 genetic algorithm runs. The ChemPLP fitness scoring function was used. For each ligand, the best scored pose was taken into consideration.

Acknowledgments

Financial support for this project was provided by the Italian Ministero dell'Università e della Ricerca (MIUR), under the National Interest Research Projects framework (PRIN_2010_5YY2HL).

Declaration of interest

The authors report no declarations of interest

References

(1) Pacher P, Batkai S, Kunos G. The endocannabinoid system as an emerging target of pharmacotherapy. Pharmacol Rev 2006;58:389-462.

(2) Di Marzo V. The endocannabinoid system: its general strategy of action, tools for its pharmacological manipulation and potential therapeutic exploitation. Pharmacol Res 2009;60:77-84.

(3) Labar G, Wouters J, Lambert D M. A review on the monoacylglycerol lipase: at the interface between fat and endocannabinoid signalling. Curr Med Chem 2010;17:2588-2607.

(4) Saario S M, Poso A, Juvonen R O, Jarvinen T, Salo-Ahen O M. Fatty acid amide hydrolase inhibitors from virtual screening of the endocannabinoid system. J Med Chem 2006;49:4650-4656.

(5) Mulvihill M M, Nomura D K. Therapeutic potential of monoacylglycerol lipase inhibitors. Life Sci 2013;92:492-497.

(6) Nomura D K, Morrison B E, Blankman J L, Long J Z, Kinsey S G, Marcondes M C, Ward A M, Hahn Y K, Lichtman A H, Conti B, Cravatt B F. Endocannabinoid hydrolysis generates brain prostaglandins that promote neuroinflammation. Science 2011;334:809-813.

(7) Kinsey S G, O'Neal S T, Long J Z, Cravatt B F, Lichtman A H. Inhibition of endocannabinoid catabolic enzymes elicits anxiolytic-like effects in the marble burying assay. Pharmacol Biochem Behav 2011;98:21-27.

(8) Ramesh D, Ross G R, Schlosburg J E, Owens R A, Abdullah R A, Kinsey S G, Long J Z, Nomura D K, Sim-Selley L J, Cravatt B F, Akbarali H I, Lichtman A H. Blockade of endocannabinoid hydrolytic enzymes attenuates precipitated opioid withdrawal symptoms in mice. J Pharmacol Exp Ther 2011;339:173-185.

(9) Kopp F, Komatsu T, Nomura D K, Trauger S A, Thomas J R, Siuzdak G, Simon G M, Cravatt B F. The glycerophospho metabolome and its influence on amino acid homeostasis revealed by brain metabolomics of GDE1(-/-) mice. Chem Biol 2010;17:831-840.

(10) Long J Z, Li W, Booker L, Burston J J, Kinsey S G, Schlosburg J E, Pavon F J, Serrano A M, Selley D E, Parsons L H, Lichtman A H, Cravatt B F. Selective blockade of 2-arachidonoylglycerol hydrolysis produces cannabinoid behavioral effects. Nat Chem Biol 2009;5:37-44.

(11) Aaltonen N, Savinainen J R, Ribas C R, Ronkko J, Kuusisto A, Korhonen J, Navia-Paldanius D, Hayrinen J, Takabe P, Kasnanen H, Pantsar T, Laitinen T, Lehtonen M, Pasonen-Seppanen S, Poso A, Nevalainen T, Laitinen J T. Piperazine and piperidine triazole ureas as ultrapotent and highly selective inhibitors of monoacylglycerol lipase. Chem Biol 2013;20:379-390.

(12) Muccioli G G, Labar G, Lambert D M. CAY10499, a novel monoglyceride lipase inhibitor evidenced by an expeditious MGL assay. Chembiochem 2008;9:2704-2710.

(13) Ben Ali Y, Chahinian H, Petry S, Muller G, Lebrun R, Verger R, Carriere F, Mandrich L, Rossi M, Manco G, Sarda L, Abousalham A. Use of an inhibitor to identify members of the hormone-sensitive lipase family. Biochemistry 2006;45:14183-14191.

(14) Minkkila A, Savinainen J R, Kasnanen H, Xhaard H, Nevalainen T, Laitinen J T, Poso A, Leppanen J, Saario S M. Screening of various hormone-sensitive lipase inhibitors as endocannabinoid-hydrolyzing enzyme inhibitors. ChemMedChem 2009;4:1253-1259.

(15) Patel J Z, Parkkari T, Laitinen T, Kaczor A A, Saario S M, Savinainen J R, Navia-Paldanius D, Cipriano M, Leppanen J, Koshevoy I O, Poso A, Fowler C J, Laitinen J T, Nevalainen T. Chiral 1,3,4-oxadiazol-2-ones as highly selective FAAH inhibitors. J Med Chem 2013;56:8484-8496.

(16) Kasnanen H, Minkkila A, Taupila S, Patel J Z, Parkkari T, Lahtela-Kakkonen M, Saario S M, Nevalainen T, Poso A. 1,3,4-Oxadiazol-2-ones as fatty-acid amide hydrolase and monoacylglycerol lipase inhibitors: Synthesis, in vitro evaluation and insight into potency and selectivity determinants by molecular modelling. Eur J Pharm Sci 2013;49:423-433.

(17) Erlenmeyer E. Ueber die Condensation der Hippursäure mit Phtalsäureanhydrid und mit Benzaldehyd. Ann Chim Pharm 1893;275:1-8.

(18) Plöchl J. Über einige Derivate der Benzoylimdozimtsäure. Ber 1884;17:1616-1624.

(19) Rao Y S. Reactions in polyphosphoric acid. I. New stereospecific synthesis of the E isomers of 2-phenyl-4-arylmethylene-2-oxazolin-5-ones. J Org Chem 1976;41:722-725.

(20) Miyaura N, Suzuki A. Palladium-Catalyzed Cross-Coupling Reactions of Organoboron Compounds. Chem Rev 1995;95:2457-2483.

(21) Weber V, Rubat C, Duroux E, Lartigue C, Madesclaire M, Coudert P. New 3- and 4-hydroxyfuranones as anti-oxidants and anti-inflammatory agents. Bioorg Med Chem 2005;13:4552-4564.

(22) King A R, Lodola A, Carmi C, Fu J, Mor M, Piomelli D. A critical cysteine residue in monoacylglycerol lipase is targeted by a new class of isothiazolinone-based enzyme inhibitors. Br J Pharmacol 2009;157:974-983.

(23) Tuccinardi T, Granchi C, Rizzolio F, Caligiuri I, Battistello V, Toffoli G, Minutolo F, Macchia M, Martinelli A. Identification and characterization of a new reversible MAGL inhibitor. Bioorg Med Chem 2014;22:3285-3291.

(24) Nomura D K, Long J Z, Niessen S, Hoover H S, Ng S W, Cravatt B F. Monoacylglycerol lipase regulates a fatty acid network that promotes cancer pathogenesis. Cell 2010;140:49-61.

(25) Verdonk M L, Cole J C, Hartshorn M J, Murray C W, Taylor R D. Improved protein-ligand docking using GOLD. Proteins 2003;52:609-623.

(26) Chanda P K, Gao Y, Mark L, Btesh J, Strassle B W, Lu P, Piesla M J, Zhang M Y, Bingham B, Uveges A, Kowal D, Garbe D, Kouranova E V, Ring R H, Bates B, Pangalos M N, Kennedy J D, Whiteside G T, Samad T A. Monoacylglycerol lipase activity is a critical modulator of the tone and integrity of the endocannabinoid system. Mol Pharmacol 2010;78:996-1003.

(27) Schlosburg J E, Blankman J L, Long J Z, Nomura D K, Pan B, Kinsey S G, Nguyen P T, Ramesh D, Booker L, Burston J J, Thomas E A, Selley D E, Sim-Selley L J, Liu Q S, Lichtman A H, Cravatt B F. Chronic monoacylglycerol lipase blockade causes functional antagonism of the endocannabinoid system. Nat Neurosci 2010;13:1113-1119.

(28) Busquets-Garcia A, Puighermanal E, Pastor A, de la Torre R, Maldonado R, Ozaita A. Differential role of anandamide and 2-arachidonoylglycerol in memory and anxiety-like responses. Biol Psychiatry 2011;70:479-486.

(29) Chen R, Zhang J, Wu Y, Wang D, Feng G, Tang Y P, Teng Z, Chen C. Monoacylglycerol lipase is a therapeutic target for Alzheimer's disease. Cell Rep 2012;2:1329-1339.

(30) *Maestro*, version 9.0; Schrödinger Inc: Portland, OR, 2009.

(31) *Macromodel*, version 9.7; Schrödinger Inc: Portland, OR, 2009.

(32) Bertrand T, Auge F, Houtmann J, Rak A, Vallee F, Mikol V, Berne P F, Michot N, Cheuret D, Hoornaert C, Mathieu M. Structural Basis for Human Monoglyceride Lipase Inhibition. J Mol Biol 2010;396:663-673.

(33) Mileni M, Kamtekar S, Wood D C, Benson T E, Cravatt B F, Stevens R C. Crystal structure of fatty acid amide hydrolase bound to the carbamate inhibitor URB597: discovery of a deacylating water molecule and insight into enzyme inactivation. J Mol Biol 2010;400:743-754.